# DIAGNOSTICS OF AN APPLIED FIELD MPD THRUSTER

**M. Andrenucci*, V. Antoni**, M. Bagatin**, C.A. Borghi°, M.R. Carraro°, R. Cavazzana**, A. Cristofolini°,R. Ghidini°, F. Paganucci*, P. Rossetti*, G. Serianni**, M. Zuin****

* Department of Aerospace Engineering, Univ. of Pisa / Centrospazio, Via A. Gherardesca 5, 56014 Pisa
** RFX Consortium, Association Euratom-ENEA on Fusion, Corso Stati Uniti 4, 35127 Padova
° Department of Electrical Engineering, University of Bologna, Viale Risorgimento 2, 40136 Bologna

## ABSTRACT

The paper describes the results of a wide experimental investigation on the critical regimes of a gas-fed, applied field Magneto-Plasma-Dynamic thruster (also said Hybrid Plasma Thruster, HPT), carried out in the framework of the project *Experimental Investigation on a Magneto-Plasma-Dynamics Thrusters for Space Applications*, sponsored by the Italian Ministry of the University and the Scientific Research (MURST-MIUR). The project was aimed at understanding the basic phenomena relevant to the so-called onset regime of MPD thrusters by means of an extensive experimental activity, carried out both with intrusive (electrostatic/magnetic probes) and not-intrusive (spectroscopy, plasma imaging) diagnostic techniques. For all the conditions investigated (660 mg/s of argon, power from 200 to 1000 kW, applied magnetic field from 0 to 80 mT), the plasma appears to be in full ionization condition, inside the thruster and in the region close to the thruster exit. At the highest power levels, in the region near the exit, a significant presence of ArIII has been observed. Probe diagnostics have allowed to identify a class of instabilities, characterized by a frequency peak and a well defined azimuthal periodicity. The results seem to indicate an electromagnetic nature of the fluctuations and their magneto-acoustic origin seems highly likely. With an applied magnetic field, the imaging technique has highlighted the presence of rotating plasma structures in the plume; their characteristics and the correlation with the probe measurements are still object of study.

## INTRODUCTION

Magneto-plasma-dynamics (MPD) thrusters both with and without applied magnetic field are currently under investigation as a possible high-power electric propulsion system for space missions, like round trip to the Moon and manned mission to Mars [1]. Near-term, less ambitious missions concern the LEO-to-GEO transfer of next generation heavier satellites, considering the increasing trend of the available power on-board. For this class of missions applied-field (AF) MPD thrusters are the favorite option, since they exhibit better performance than self-induced devices at low power levels (some 10 kW).

However, at present, MPD thrusters performance tend to significantly decay above a certain current level, due to the onset of critical regimes, characterized by large fluctuations in arc voltage and plasma quantities.

The comprehension of the physical mechanisms at the origin of these fluctuations is probably mandatory in order to successfully address the development process of the MPD thrusters technology. For this reasons a two-year research project, titled *Experimental Investigation on a Magneto-Plasma-Dynamics Thrusters for Space Applications* and co-sponsored by the Italian Government, started in 2001. Through an extensive experimental campaign on plasma diagnostics in an MPD thruster, the research allowed the creation of a large database and highlighted some important dependencies between thruster operating parameters and plasma behavior, although an exhaustive analysis of all the data gathered has not completed yet.

The activity has been jointly carried out by Centrospazio (research coordinator), the RFX Consortium of Association Euratom- ENEA on Fusion and the Department of Electrical Engineering of Bologna University, as skilled centers on plasma studies.

The paper shows some of the most important results gathered during the entire project. The optical diagnostics activity is described more extensively, since another paper [2] completely devoted to the results on plasma fluctuations from probe measurements is presented at this conference.

## EXPERIMENTAL APPARATUS

The experimental device is shown in Fig.1. It is an axis-symmetric MPD thruster with an applied magnetic field (Hybrid Plasma Thruster - HPT) [3-6]. The HPT, developed at Centrospazio, consists of a hollow cathode (copper, 20 mm diameter, 50 mm length) lying on the thruster axis, through which 70-90% of a gaseous propellant is injected into the discharge chamber, and an anode, consisting of a cylinder centered on

the axis (aluminum, 200 mm inner diameter, 180 mm length). Eight straps, made of copper, divide a central chamber from a peripheral chamber. 10-30% of the propellant is injected through eight peripheral hollow electrodes (copper, 12 mm in diameter each). These electrodes can be used as auxiliary cathodes to pre-ionize the peripheral propellant by means of a secondary discharge between these cathodes and the anode.
A 70-turns coil surrounding the thruster, can generate a magnetic field up to 100 mT on the thruster axis.
The HPT thruster is mounted on a thrust stand inside the Centrospazio IV3 vacuum chamber, which maintains a back pressure of the order of $10^{-4}$ mbar during the pulse. The electric power for the HPT is generated by a Pulse Forming Network (PFN), which supplies quasi-steady current pulses during 2.5 ms. The propellant is injected by two gas feeding systems, one for the central cathode and the other for the peripheral cathodes, based on fast acting solenoid valves, which provide gas pulses with a long plateau after few milliseconds from valve activation[3]. When a steady state mass flow is reached, the discharge takes place by switching on an ignitron which closes the electric circuit. The magnetic field solenoid is powered by a DC generator, switched on few seconds before the discharge.
During the experiments described in this paper argon is utilized as propellant at a mass flow rate of 660 mg/s, distributed in the ratio of 100:10 between the central and peripheral cathodes respectively. The peripheral electrodes are not activated, while tests have been performed with and without the application of the external magnetic field. Values of the field on the thruster axis were of 40 and 80 mT.

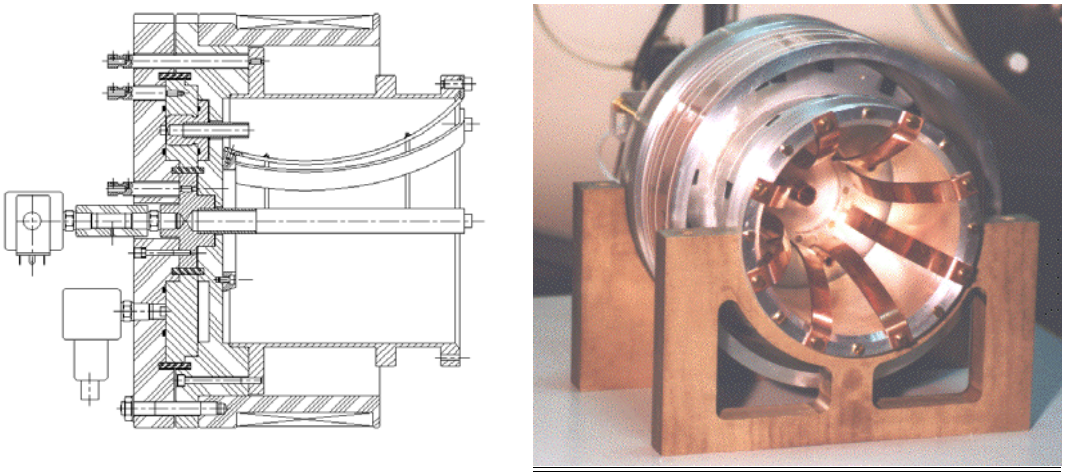

*Fig. 1*: Schematic drawing (left) and picture (right)of the thruster assembly.

## DIAGNOSTICS DESCRIPTION

### Optical diagnostics

Two optical diagnostics were utilized to characterize the plasma plume of the MPD thruster:

- The intensity of the radiation has been measured by means of an optical multi-channel analyzer. The measured spectra ranges between 300 and 1100 nm, with a constant wavelength resolution $\Delta\lambda/\lambda$ = 900. In order to avoid the strong radiation absorption which affects the plasma plume, an optical probe has been placed in the plasma. The probe has been realized by means of a fiber optic cable connected to a collimator based on an achromatic doublet geometry with a focal length of 3 cm. The whole system was encapsulated in a Pyrex glass tube of 1.2 cm diameter.
- In order to observe the structure of the plasma, images of the plume have been taken by means of a fast shutter CCD camera.

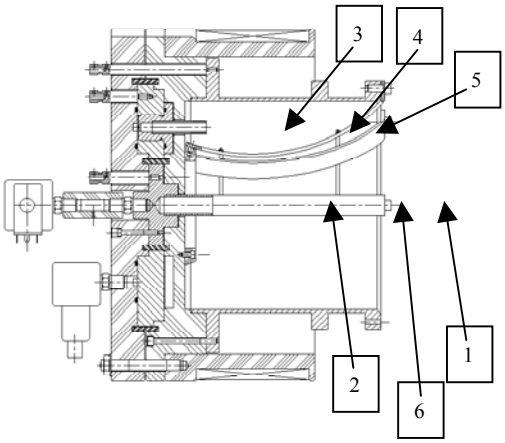


*Fig. 2*: Positions of the optical probe.

| | | (1) | | (2) | (3) | (4) | (5) | (6) | |
|---|---|---|---|---|---|---|---|---|---|
| *Discharge current* I [A] | *Impressed B Field* [mT] | Δt [ms] | Δt [ms] | Δt [ms] | Δt [ms] | Δt [ms] | Δt [ms] | Δt [ms] | Δt [ms] |
| 4500 | 0 | 0-0.25 | 0.5-0.75 | 0.5-0.55 | 0.5-1 | 0.5-1 | 0.5-1 | 0-0.5 | 0.5-1 |
| 6000 | 0 | 0-0.25 | 0.5-0.75 | 0.5-0.55 | 0.5-1 | 0.5-1 | 0.5-1 | 0-0.5 | 0.5-1 |
| 7500 | 0 | 0-0.25 | 0.5-0.75 | 0.5-0.55 | 0.5-1 | 0.5-1 | 0.5-1 | 0-0.5 | 0.5-1 |
| 4500 | 80 | 0-0.25 | 0.5-0.75 | 0.5-0.55 | 0.5-1 | 0.5-1 | 0.5-1 | 0-0.5 | 0.5-1 |
| 6000 | 80 | 0-0.25 | 0.5-0.75 | 0.5-0.55 | 0.5-1 | 0.5-1 | 0.5-1 | 0-0.5 | 0.5-1 |
| 7500 | 80 | 0-0.25 | 0.5-0.75 | 0.5-0.55 | 0.5-1 | 0.5-1 | 0.5-1 | 0-0.5 | 0.5-1 |

*Table. 1*: Time intervals utilized for the optical probe positions and thruster conditions.

The optical probe has been placed in six different positions, as shown in Fig. 2. The optical axis of the probe in position 1 through 5, was parallel to the axis of the thruster. In position 6, the optical axis was perpendicular to it. In each configuration the tests indicated on table 1 has been performed. In all of the tests conditions the Argon mass flow was 600+60 mg/s.
The imaging diagnostic was performed by means of a Pco Sensicam CCD colour fast shutter camera. The minimum exposure time is of 100 ns. Its quantum efficiency has a peak of 40% at 500 nm. As a consequence, the light recorded by the camera comes mostly from ArII. In order to evaluate the velocity of some non uniform structures in the plasma, a double exposition mode has been used.

**Probe diagnostics**

The first electrostatic system of probes used, named 'Rake' probe, consists of 7 aligned graphite electrodes, 8 mm apart from each other, and housed in a boron-nitride case (Fig. 3). The probes were used in a five-pin balanced triple probe configuration [7] to avoid phase shift problems and to obtain simultaneous measurements of electron density and temperature. The estimated analog signal bandwidth was 500 kHz, in order to obtain measurements of both average value and fluctuations of electron temperature, electron density and plasma potential. The central electrode was placed at 80 mm from the thruster outlet, along the thruster axis; with respect to this position, other measurements were performed by moving the probe by 115 mm in the direction perpendicular to the axis of the thruster.

*Fig. 3*: Picture of the assembled 'Rake' probe.

The space and time correlations of floating potential fluctuations in the plume have been investigated by a proper fluctuation probe instrument. It consists of two concentric rings of respectively 60 and 100 mm radius, each housing 32 equally spaced electrodes. Each ring had also a linear probe array along a diameter, to allow radially resolved measurements (Fig. 4). The probe system has been manufactured using printed circuit board standard technology. This also allows to simplify the electrical connections by using standard flat cables. In order to reduce the plasma perturbation, most part of the unused surface has been cut away, while the remaining one has been masked by a Boron-Nitride film. The system was placed coaxially to the thruster axis, at 80 mm from the thruster outlet.

*Fig. 4*: The assembled annular system of electrostatic probes, before the deposition of the Boron-Nitride film.

The magnetic probe system consisted of two three axes probes housed in a quartz tube spaced by 15 mm. Each probe consists of three coils wound with 0.2 mm dia wire on a small support (7 by 7 by 8 mm). In order to reduce the capacitive coupling the support has been machined to avoid any contact between the coils. The coils where connected through a coaxial cable terminated at 50 ohm to avoid capacitive resonance, allowing a flat bandwidth up to 1 MHz.

All data have been collected by connecting the probes to a digital oscilloscope (Yokogawa DL716) with 12 bit resolution isolated inputs at a sampling frequency of 10 MHz.

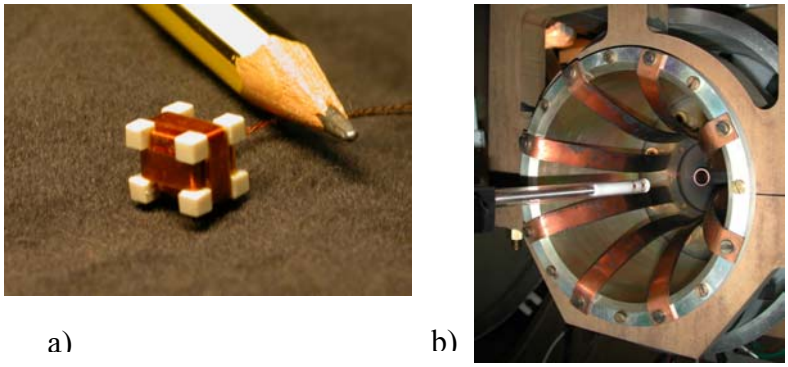

a) b)

*Fig. 5*: A single three-axes magnetic probe (a), and the magnetic system probes in the thruster (b).

## OPTICAL MEASUREMENTS

### Emitted radiation

The radiation collected by the optical probe in position 1, is dominated by the argon emission. ArIII lines are observed in the wavelength range of 320-350 nm, ArII lines in the range of 350-500 nm and ArI lines in the range of 690-900 nm. The intensity of the ArIII lines is comparable with ArII lines. The intensity of ArI lines

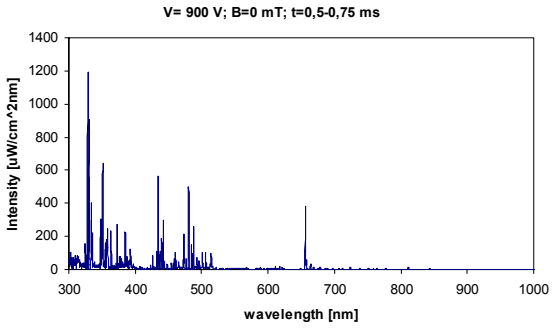


*Fig. 6*: Emission spectrum recorded in position 1 at Δt = 0.5-0.75 ms, B = 0 mT, I = 4500 A.

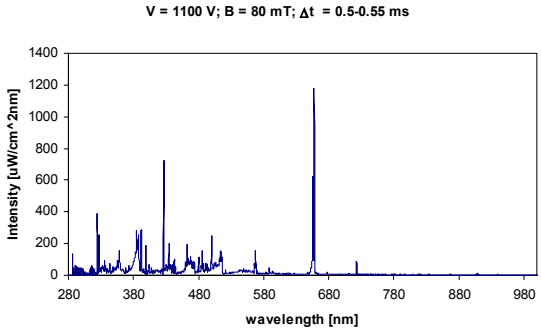


*Fig. 7*: Emission spectrum recorded in position 2 at Δt = 0.5-0.55 ms, B = 80 mT, I = 6000 A.

are very low. Other emission lines of different elements has been recorded. Emission from oxygen and nitrogen are due to residual air in the vacuum chamber. The presence of copper is due to electrodes erosion. Hydrogen and carbon are contained in the oil of diffusion pumps and/or in the insulator plate (made of pexiglass). In figure 6 the emission spectrum recorded in position 1 at a discharge current of 4500 A, without an externally applied magnetic field, in the time interval Δt = 0.5-0.75 ms, is shown.

Due to the impurities contained in the plasma, the formation of a coat on the glass surface of the optical probe has been observed. The progressive degradation of the probe transparency caused difficulties in evaluating the variation of the emitted radiation for different thruster conditions.

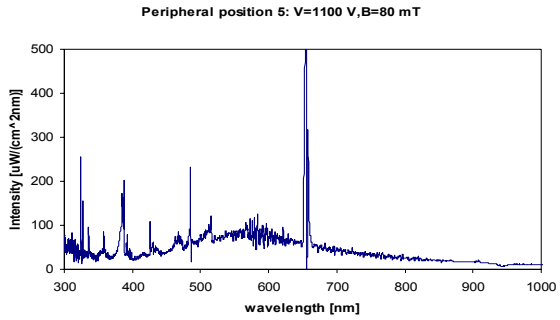


*Fig. 8*: Emission spectrum recorded in position 6 at Δt = 0.5-0.55 ms, B = 80 mT, I = 6000 A.

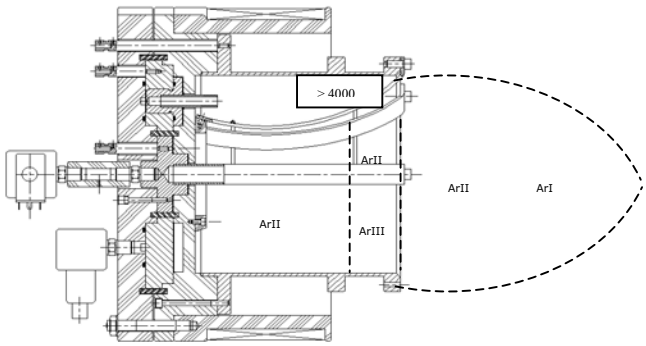


*Fig. 9*: Qualitative scheme of the emission regions of the thruster

Intense carbon and copper lines has been recorded with the optical probe placed inside the thruster both on the axis and in peripheral positions (position 2,3,4,5 in figure 2). In these optical configurations, the observed emission lines are due mainly to ArII. Lines of ArIII and ArI with a low intensity have been only measured at high values of current. Figure 7 shows a spectrum measured on the axis at I = 6000 A, B = 80 mT, in the time interval Δt = 0.5-0.55 ms in position 2.
In figure 8 the radiation measured in the peripheral position (position 6) is shown. The operating conditions in this case are: B = 80 mT and I = 6000 A. The continuum emission is an important contribution to the total radiation. Continuum emission can be observed only in front of the central cathode and of the anodic straps. Thus, it should derive from the copper vapor.
Due to the absence of ArI lines it can be concluded that inside the thruster the plasma is fully ionized both at low and high currents. The lines of Ar III lines are only present near the outlet of the thruster. A qualitative scheme of the emission is presented in figure 9.

**Evaluation of the excitation temperature**
An estimation of the excitation temperature has been done by means of ArII and ArIII emission lines. Due to the overlapping of other elements (carbon and copper) with Ar lines, the Boltzmann plot has been only obtained from the radiation recorded with the probe in position 1. In figure 10 the Boltzmann plot for the case of I = 4500 A, B = 0 mT, in the time interval Δt = 0.5-0.75 ms, is shown.
It is possible to divide the energy level system of ArII into two parts: high energy levels, characterized by an high value of temperature $T_H$, and low energy levels, characterized by a low temperature $T_P$. The population of the high energy levels is dominated by collisional processes, and is not affected by radiative decay processes. Therefore the temperature $T_H$ can give a reliable estimation of the electronic temperature. In figure 11, the variation of $T_H$ with the discharge current and with the externally applied magnetic field, in the time intervals Δt = 0-0.25 ms (11.a) and Δt = 0.5-0.75 ms (11.b), is shown.

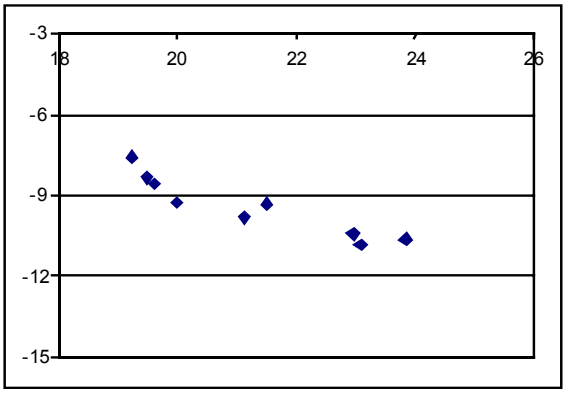


| *Line* λ [nm] | $E_{up}$ E [eV] |
|---|---|
| 480.602 | 19.22 |
| 434.806 | 19.49 |
| 433.120 | 19.61 |
| 457.935 | 19.97 |
| 460.956 | 21.14 |
| 448.181 | 21.50 |
| 358.844 | 22.95 |
| 397.936 | 23.08 |
| 399.479 | 23.85 |

*Fig. 10*: Boltzmann plot of the ArII system at I = 4500 A, B = 0 mT and Δt = 0.5-0.75 ms. Lines wavelength and upper energy level are reported as well.

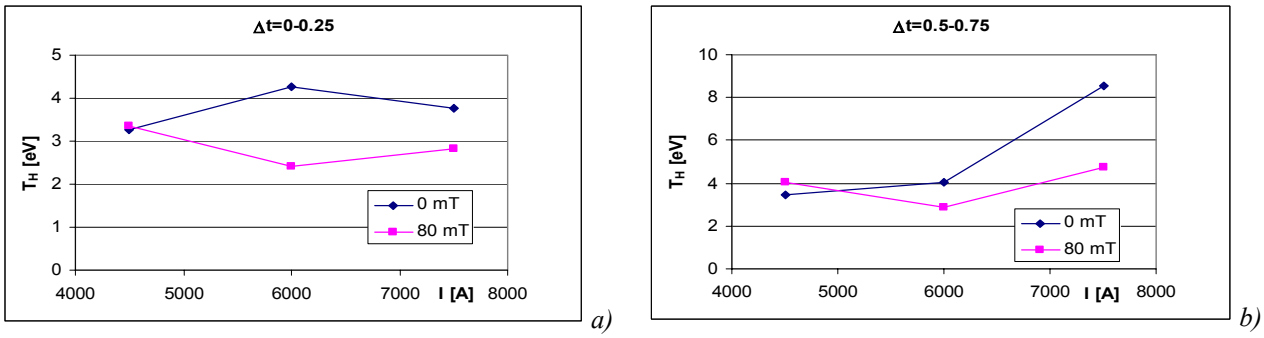


a) b)

*Fig. 11*: Temperature $T_H$ vs discharge current at different values of applied B in the start-up phase (11.a) and stationary phase (11.b).

The wavelength of the high levels is out of the spectrograph range (< 300 nm). Therefore only the excitation temperature $T_P$ between the low levels is calculated. Figure 12 shows the variations of $T_P$ with discharge current and external applied magnetic field, in the time intervals Δt = 0-0.25 ms (on the left) and Δt = 0.5-0.75 ms (on the right). Without an externally applied magnetic field, the temperature increases by increasing discharge currents. When the applied magnetic field B is switched on, $T_P$ appears to be higher at low values of the current. The results are in contrast with what it is found with the ArII system. In the present case, only low ArIII levels are considered and the lines are measured in wavelength range (320-350 nm) where the CCD sensibility is weak.

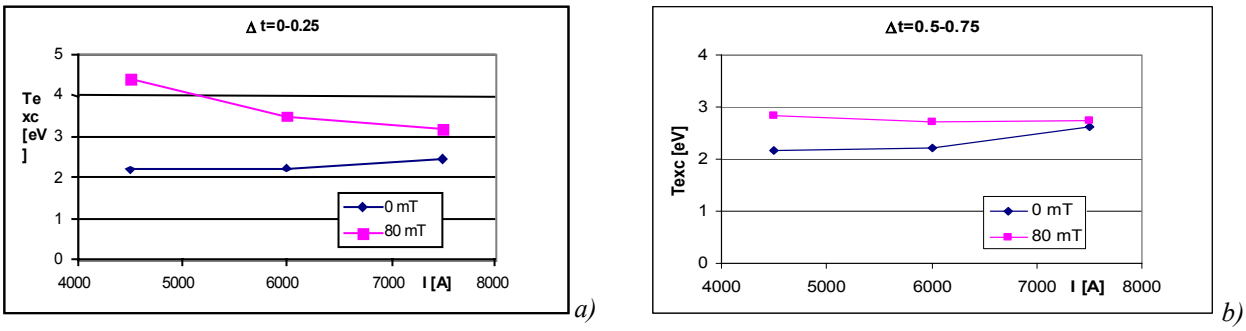


a) b)

*Fig. 12*: Temperature $T_P$ vs discharge current at different values of applied B in the start-up phase (12.a) and stationary phase (12.b).

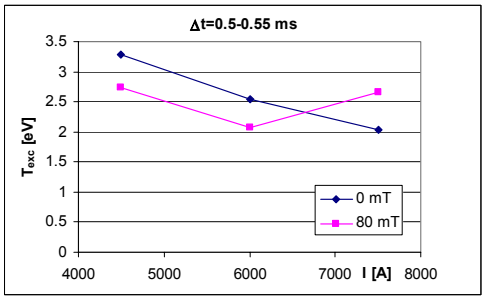


*Fig. 13*: Temperature $T_{exc}$ vs discharge current at different values of applied B in the interval time Δt = 0.5-0.55 ms.

The radiations measured with the optical probe inside the thruster (position 2, 3, 4 and 5) are strongly affected by carbon and copper emissions. An indication of the excitation temperature $T_{exc}$ between two or a few levels (typically four or five in the range of 19-23 eV) of ArII could be derived. In figure 13 the variations of $T_{exc}$, with the probe in position 2, in the time interval Δt = 0.5-0.55 ms, is shown. The temperature decreases with a decreasing current. In figure 14 the variation of excitation temperature with different currents, evaluated with the probe in the peripheral positions indicated in figure 2 (position 3, 4 and 5), is shown.

In position 4 (figure 14.b) $T_{exc}$ increases with increasing discharge currents and applied magnetic fields. In position 5 (figure 14.c) $T_{exc}$ decreases with decreasing currents. The application of external B does not affect the temperature. This is probably due to the observed region very close to the electrode where the applied magnetic field is negligible when compared to the self-induced magnetic field.

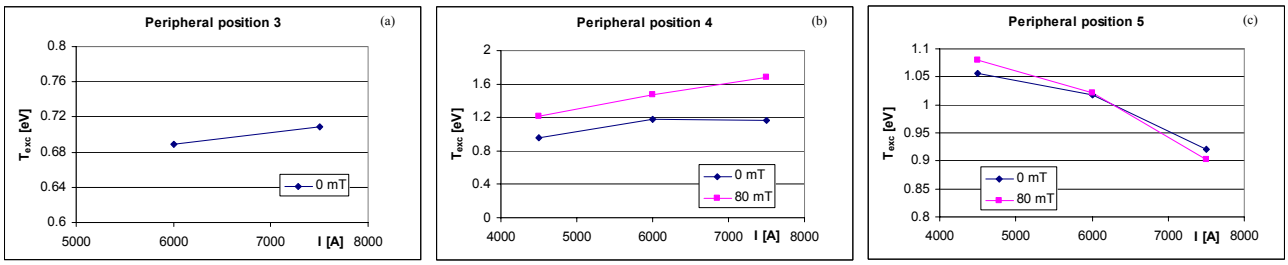


*Fig. 14*: Temperature $T_{exc}$ vs discharge current at different values of applied B in the interval time $\Delta t$ = 0.5-0.55 ms. (a) position 3, (b) position 4, (c) position 5.

**Plasma imaging**

The imaging of the plasma plume was performed only in two conditions:

*1. Test condition: I = 7500 A, B = 0 mT*

During the stationary and start up phase the plasma plume appears to be uniform as shown in figure 15 and 16. However, there are some non-uniformity in the region near the outlet of the thruster. Particles, probably of copper due to electrode erosion, flowing out of the thruster, are observed.

*Fig. 15*: Plasma plume in regime conditions registered with $t_{exp}$ = 5 μs and $t_d$ = 1 ms.

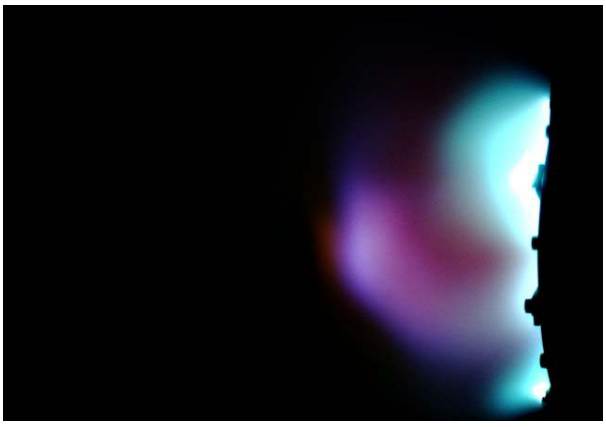

*Fig. 16*: Plasma plume starting up, registered with $t_{exp}$ = 6 μs and $t_d$ = 50 μs.

*2. Test condition: I = 7500 A, B = 80 mT*

Start up phase: The plasma plume imaging during the start up phase is shown in figures 17-20. During this phase a plasma clot is flowing out of the thruster with velocity of about 3.3 km/s. The clot radial dimension is about 8-12 cm. Its intensity decreases during its flow. The clot drags some plasma filaments with an helicoidal structure which follow the lines of the magnetic field. Some peripheral striations are also present at the exit of the thruster. In fig. 18 the magnetic field lines, calculated by means of a two dimensional electromagnetic code, are placed on the plasma plume image. This is to show that the striations follow the lines of the field. These striations are also observed during the regime condition.

*Fig. 17*: Plasma "clot" during the expulsion from thruster with $t_{exp}$ = 10 µs and delay $t_d$ = 25 µs.

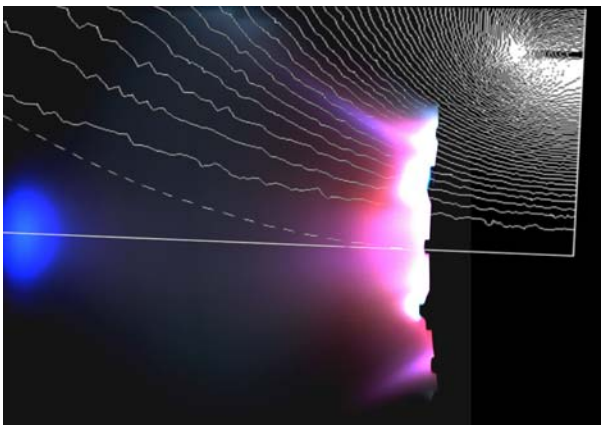

*Fig. 18*: Plasma striations with $t_{exp}$ = 5µs and delay $t_d$ = 100 µs.

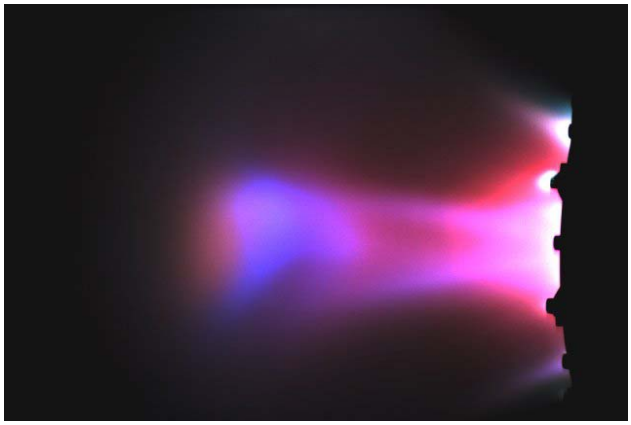

*Fig. 19*: Plasma plume with $t_{exp}$ = 10µs and delay $t_d$ = 50 µs. Plasma "clot" after the expulsion. Two striations from the centre of thruster reach the clot boundary.

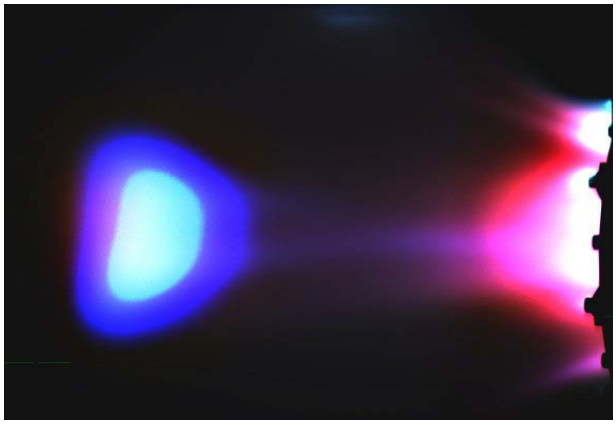

*Fig. 20*: Plasma plume with $t_{exp}$ = 10µs and delay $t_d$ = 75 µs.

Regime phase: In this condition two different types of striations are observed. The peripheral ones, which are also present during the start up phase, and the central ones. The central are moving and have a thickness of 3 – 6 cm. They appear to be similar to the structures following the clot at the start up of the thruster operation. The plasma plume images of the regime phase are shown in figures 21 and 22.

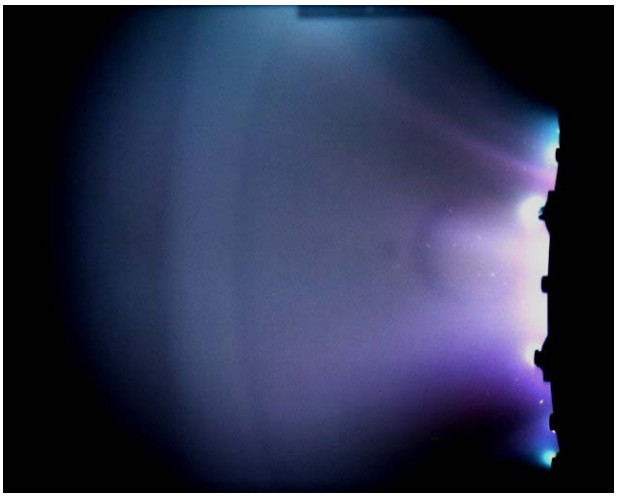

*Fig. 21*: Plasma plume with $t_{exp}$ = 2.5µs, $t_d$ = 1 ms. The post-processing treatment is exactly the same of fig. 20.

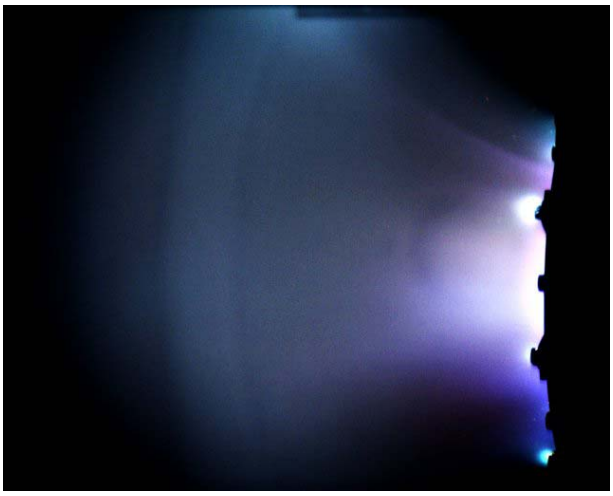

*Fig. 22*: Plasma plume with $t_{exp}$ = 2.5µs, $t_d$ = 1 ms. The post-processing treatment is exactly the same of fig. 19.

## PROBE MEASUREMENTS

Magnetoplasmadynamic instabilities are suspected to favor, or even cause the 'onset' phenomenon, limiting the development of highly efficient plasma accelerators.

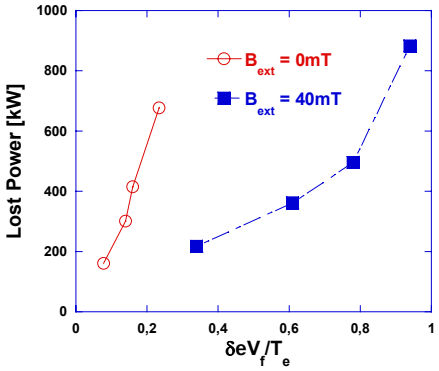


*Fig. 23*: Lost Power vs fluctuation levels of floating at different Bext, as functions of current.

In order to understand the role of plasma fluctuations in the deterioration of the overall performance an investigation of the mean and fluctuating plasma parameters such as electron density and temperature, and floating potential has been performed by means of the different electrostatic and magnetic probe systems above described. The performance can be improved by adding an external magnetic field. In the thruster under examination it is generally found that the improvement due to the applied field is considerably large only at low current regimes [5,6]. Our experiments have shown how these phenomena are related to the appearance of large plasma fluctuations. The lost power increases with increasing fluctuation levels, both with and without the applied external magnetic field (Fig. 23).

The mean values of electron temperature and density in the plume of the thruster have been measured, in different operating conditions. Density is typically of the order of some $10^{20}$particle/$m^3$, with a tendency to peaking with increasing current. The application of the external magnetic field $B_{ext}$ flattens the profiles. The electron temperature spans from 3 to 5 eV without the external magnetic field, and from 6 to 9 eV when this is applied.

The study of the electrostatic fluctuations has been addressed to characterize the regimes with and without external field and in particular the onset of the critical conditions at high power. These regimes have shown high levels of fluctuations in electrostatic signals measuring plasma parameters, such as temperature, density, and floating potential. The root mean square amplitude of the fluctuations increases with the current, and grows to higher values when the external magnetic field is applied.

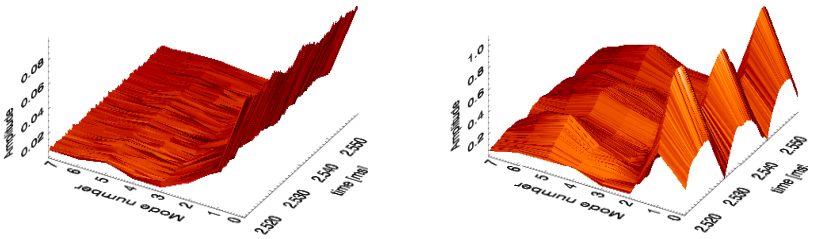


***a)*** ***b)***

*Fig. 24*: Mode amplitude time evolution of floating potential at $I_{discharge}$=4.2 kA: a) $B_{ext}$=0 mT; b) $B_{ext}$=40 mT.

Power spectra of the floating potential signals are characterized by the presence of a clear peak, whose frequency increases almost linearly with the current, spanning in the range between 40 and 70 kHz. These frequencies slightly grow with the application of the external magnetic field, up to 90 kHz. An annular system of probes has been realized to achieve information in space and time correlations properties. At low currents, in absence of external magnetic field, only a global m=0 mode can be revealed. The application of $B_{ext}$ causes the development of an azimuthal m=1 mode (fig. 24). This can be seen also without $B_{ext}$, but only at the highest currents.

To these frequencies are associated phase velocities spanning from 10 to 35 km/s, rather close to the Alfvén velocity in the plasma under investigation ($v_A=B/(\mu_0\rho)^{1/2}$, where ρ is the mass density of the used gas).

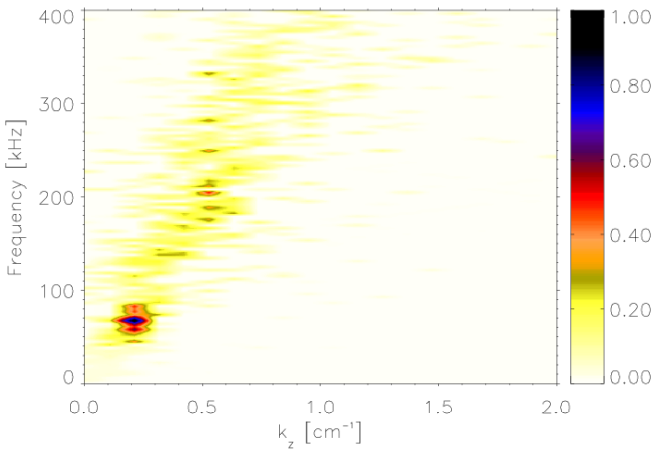


*Fig. 25*: Experimental dispersion relation (S(k,f)) of the magnetic fluctuations for $I_{discharge}$= 8.2 kA.

Magnetic measurements at high frequencies in the inner part of the thruster have revealed large amplitude fluctuations, increasing with current, up to 35% of the mean magnetic field. In

particular, their power spectra have shown peaks in same range as the electrostatic spectra. A double point analysis on the signals of radial and axial magnetic field has shown an almost constant phase difference of $\pi/2$. This means circular polarization (right) of the fluctuations in the plane r-z. The obtained wavenumbers in the axial directions again imply phase velocity that is comparable with the Alfvén velocity (Fig. 25). The 'Alfvénic' nature of these instabilities is actually under investigation and more extensively treated in [2].

## CONCLUSIONS

The activity described in the paper represents a first attempt to join different, high skilled Italian groups involved in plasma physics to study the critical operation regime of an applied field MPD thruster, by means of both electromagnetic probes and optical techniques. Although the data gathered during seven test campaigns have not completely analyzed yet, some conclusions can be already drawn:

- for all the conditions investigated, the plasma appears to be in full ionization condition, inside the thruster and in the region close to the thruster exit;
- At the highest power levels, in the region near the exit, a significant presence of ArIII has been observed;
- Plasma is contaminated by products coming from electrode and insulator erosion (copper, carbon and hydrogen) and perhaps from the oil of the vacuum pumping system;
- A correlation between the fluctuation amplitude of the plasma quantities and a significant percentage of the power lost has been found;
- A class of instabilities has been identified. The instabilities are characterized by a frequency peak and a well defined azimuthal periodicity;
- The results seems to indicate an electromagnetic nature of the fluctuations and their magneto-acoustic origin seems highly likely;
- With an applied magnetic field, rotating plasma structures, have been observed; their characteristics and the correlation with the probe measurements are still object of study.

## ACKNOWLEDGEMENT

The activity has been mainly carried out in the framework of a COFIN project, co-sponsored by the Italian Ministry for the University and the Scientific Research (MURST-MIUR).

## REFERENCES

1. P. Rossetti et al., "Propulsion 2000 Phase II- Feasibility Study and Pre-proposal Analysis", CS/P2000/FR-002/PR, Centrospazio, Jan. 2003.

2. M. Zuin et al., *Plasma Fluctuations in an MPD Thruster with and without the Application of an External Magnetic Field,* IEPC-03-0299, 28th International Electric Propulsion Conference, March 17-21, Toulouse, France

3. V.B. Tikhonov et al., *Investigation on a New Type of MPD Thruster*, OR 21, 27th European Physical Society Conference on Controlled Fusion and Plasma Physics, 12-16 June 2000, Budapest, Hungary, 12-16 June 2000.

4. V.B. Tikhonov et al., *Development and Testing of a New Type of MPD Thruster*, IEPC-01-123, 27th International Electric Propulsion Conference, October 14-19, 2001, Pasadena, CA.

5. F. Paganucci et al., *Performance of an Applied Field MPD Thruster*, IEPC-01-132, 27th International Electric Propulsion Conference, October 14-19, 2001, Pasadena, CA.

6 P. Rossetti et al., "*Performance of an Applied Field MPD Thruster with a Pre-ionization Chamber*", AIAA-2002-2103, 33rd Plasmadynamics and Lasers Conference, May 20-23, 2002, Maui, Hawaii.

7 H. Y. Tsui et al., Rev. Sci. Instrum. **63**, 4608 (1992).